Ionization of hydrogen atoms by circularly polarized microwaves

Robert Gębarowski[1] and Jakub Zakrzewski[1,2]
[1]*Instytut Fizyki Uniwersytetu Jagiellońskiego, ulica Reymonta 4, 30-059 Kraków, Poland*
[2]*Laboratoire Kastler-Brossel, Université Pierre et Marie Curie, T12, E1, 4 place Jussieu, 75272 Paris Cedex 05, France*
(Received 17 May 1994)

Ionization of hydrogen Rydberg atoms by *circularly* polarized microwaves is studied numerically within the framework of classical mechanics. Both the simplified two-dimensional model (in which the plane of polarization coincides with the orbit plane) and a fully three-dimensional system are considered. It is shown that the ionization proceeds in the diffusive manner for all microwave frequencies except the low-frequency limit. The threshold for diffusive excitation as well as the diffusion speed is strongly dependent on the initial state of the system for smooth pulse excitation. In a high-frequency limit the ionization threshold rises sharply—the atom is much more resistant to the excitation. Two distinct regimes of stabilization windows (regions where ionization decreases with increasing field amplitude), one in the strong short-laser-pulse domain and the other in the weak microwave domain are identified and discussed.

PACS number(s): 32.80.Rm, 42.50.Hz, 34.50.Gb, 05.45.+b

I. INTRODUCTION

The pioneering experimental study of ionization of highly excited hydrogen atoms by linearly polarized microwaves (LPM) [1] was the beginning of an intensive study of the problem in the past twenty years. The first theoretical understanding of the ionization process was obtained [2] using Monte Carlo classical simulations, associating the ionization threshold with the onset of classical chaos in the system. Since then a great number of contributions appeared which treated the problem either classically or quantum mechanically at various degrees of approximation. At the same time improved experiments provided a stimulus and new puzzles for the theory (for recent reviews of the theory see [3–7]; experimental details may be found in [9,10]).

It has now become common knowledge that the frequency dependence of the threshold in LPM ionization may be roughly divided into a few regions characterized by distinct features. The relevant parameter is the ratio of the microwave frequency ω to the Kepler frequency on the initial orbit ω_K. For the scaled frequency $\omega_0 = \omega/\omega_K \ll 1$, the quasistatic limit is realized, the classical ionization is due to over barrier escape (like in the static, homogeneous electric field), and quantum corrections are due to tunneling (which may be taken into account semiclassically using, e.g., the complex path method [8]). For higher frequencies (but still for $\omega_0 < 1$), the onset of classical chaos and the breakup of Kol'mogorov-Arnol'd-Moser tori well approximate the quantum ionization threshold; the diffusive gain of energy by an electron is a main mechanism leading to ionization with additional modifications due to classical resonances. The agreement between classical and quantum predictions breaks up for $\omega_0 > 1$; the quantal thresholds are significantly higher due to the phenomenon of quantum localization, analogous to Anderson localization in disordered solids. It is this frequency domain that received most experimental and theoretical attention in recent years [3–7,9,10] in relation to "quantum chaos" studies and the semiclassical limit.

Much less is known about the ionization process in the presence of *circularly* polarized microwaves (CPM). Despite early analysis [11,12], the systematic studies are only beginning to emerge [13–20]. Experimental setups used for hydrogen ionization in LPM have to be significantly modified to allow for CPM excitation. The experiments carried out for alkali-metal atoms by Gallagher and co-workers [21,22] have clearly shown the importance of the nonhydrogenic core; thus their results cannot substitute for hydrogen studies. On the other hand, a detailed theoretical, both classical and quantum, analysis may be carried out practically only for hydrogen. Fortunately, just now experiments with hydrogen atom ionization by circularly polarized microwaves are in progress [23]; this makes the theoretical analysis of the process timely and important.

There is a basic difference between ionization by LPM and CPM. In the former case the projection of the angular momentum on the polarization axis is conserved; thus the problem considered is effectively a two-dimensional one. On the contrary, the CPM ionization requires, in principle, the treatment of a fully three-dimensional system since no constant of motion is known to exist (except for the approximate one in the purely perturbative regime [24]). Fortunately, significant insight may be obtained from simplified lower-dimensionality models. Again, the situation is much simpler for the LPM case where the simplest atomic model may be one dimensional. Such a model may be quite useful for initial states extended along the polarization axis [4–7]. For the CPM ionization problem the simplest model is two dimensional. Here the electron motion is confined to the polarization plane. In fact, most of the studies of the problem assumed such a configuration [13,14,16–19].

Even then quite contradictory predictions have been obtained, e.g., for low-frequency ionization threshold behavior [13,21,22]. This regime was considered in most of the theoretical analyses. The controversy has been resolved very recently [18,19]. The motion in this regime is mainly regular. However, since even the most simplified model is two dimensional, the ionization threshold is strongly dependent on the initial state (and/or on the choice of the left or right circularly polarized radiation), as shown in [17] (see also a detailed study of the low-frequency regimes in [19]). This sensitivity was confirmed by the only quantum analysis performed up until now [18].

Much less is known about the ionization process (in CPM) for higher-frequency regimes. The classical Kepler map analysis [14], performed at a frequency $\omega_0 = -1$, suggests that the electron motion, at least for circular or low eccentricity initial states is quite regular. For the high-frequency regime $\omega_0 > 1$, important domains of highly chaotic nearly circular orbits have been obtained in [16]. There a diffusive character of ionization has been stressed and the ionization thresholds has been estimated by the resonance overlap criterion. It is most important to obtain reliable classical information about the ionization threshold and the mechanism of the classical ionization for comparison with the quantum studies. Since the process of ionization in CPM is three dimensional, it is by no means clear whether the localization phenomenon, which dominated the LPM ionization studies in recent years, may be observed in CPM ionization. Recall that in solids, an analogous Anderson localization is strongly dependent on the dimensionality of the problem.

Due to technical difficulties there is still a long way to go before a full understanding of the ionization of hydrogen in CPM will be obtained. The aim of this paper is to provide understanding of the classical features of the ionization by means of a detailed numerical study. We concentrate mainly on the ionization of hydrogen prepared initially in well defined circular or elliptical states. This is motivated by recent advances in the preparation of such Rydberg states, e.g., by the crossed fields method [25,26]. In that way states strongly oriented in space are produced. If the microwave polarization plane is chosen to match the initial states orientation, a simplified two-dimensional model of the ionization should be a good approximation of the truly three-dimensional situation.

The paper is organized as follows. The model and the numerical methods used are described in Sec. II. In Sec. III numerical estimates for the ionization thresholds are presented for different simulations of the initial states. The importance of the shape of the microwave pulse is pointed out. The analysis is mainly carried out in the simplified two-dimensional model, although we discuss also fully three-dimensional system and, in particular, different initial orbit orientations with respect to the polarization plane. Finally, the conclusions and future perspectives form the content of Sec. IV.

II. THE THEORETICAL APPROACH

We shall consider the following classical Hamiltonian describing, in the dipole approximation and in atomic units, the hydrogen atom in the field of the circularly polarized radiation

$$H = \frac{p_x^2 + p_y^2 + p_z^2}{2} - \frac{1}{r} - Ff(t)\left[x\cos(\omega t + \varphi) + y\sin(\omega t + \varphi)\right], \tag{2.1}$$

where $r = \sqrt{x^2 + y^2 + z^2}$ and F, ω, and φ are the maximal amplitude, the frequency, and the initial phase of the microwave field, respectively. Note that a change in the sign of ω is equivalent to a change from right CPM to left CPM. We shall explore this possibility below and allow ω to take both positive and negative values to study both types of polarization. In (2.1) $f(t)$ describes the microwave pulse shape chosen to represent "flat-top" pulses, as realized, e.g., in experiments by Koch [9],

$$f(t) = \begin{cases} \sin^2(\pi t/2\tau), & 0 < t < \tau \\ 1, & \tau < t < T - \tau \\ \cos^2\{\pi[t - (T-\tau)]/2\tau\}, & T - \tau < t < T \\ 0 & \text{elsewhere.} \end{cases} \tag{2.2}$$

T and τ describe the pulse duration and its rise (and falloff) time, respectively. Note that in the limit $\tau \to 0$ we may recover the square pulse (resulting in the monochromatic field for $T \to \infty$), while $T = 2\tau$ corresponds to a smooth, sine-squared pulse which may well approximate the microwaves in the experiments by Bayfield and Sokol [10]. Such a pulse may be used also for classical simulations of short intense laser pulse excitation [27].

The Hamiltonian (2.1) depends on four quantities (ω, F, T, τ) and the initial electron energy E, yielding the fifth parameter (we shall always average the results of numerical simulations over the initial field phase φ). However, the electron motion depends only on four independent parameters since the hydrogen atom in an external field obeys the scaling property [28]. Explicitly, the motion is invariant under the scale transformation

$$\begin{aligned} H &\to \lambda H, \\ x, y, z &\to \lambda^{-1}x, \lambda^{-1}y, \lambda^{-1}z, \\ p_i &\to \lambda^{1/2}p_i, \\ t, T, \tau &\to \lambda^{-3/2}t, \lambda^{-3/2}T, \lambda^{-3/2}\tau, \\ \omega &\to \lambda^{3/2}\omega, \\ F &\to \lambda^2 F, \end{aligned} \tag{2.3}$$

for arbitrary real λ. Suppose that we are interested in excitation of the electron with initial energy $E_n = -1/2n^2$ by a field of amplitude $\mathcal{F}$ and frequency Ω. Choose $\lambda = n^2$ and the scaling above; the resulting initial *scaled* energy will be $E = -1/2$, the scaled field frequency $\omega = \Omega n^3$, and the field amplitude $F = \mathcal{F}n^4$. The scaled frequency is nothing but the ratio of the unscaled frequency to the Kepler frequency $\omega_K = (-2E_n)^{3/2}$. Scaled quantities are sometimes denoted by a subscript 0 in the literature [3]. We shall not use the additional subscript assuming from now on that *all* parameters are expressed

in scaled variables.

All previous classical studies of the problem [13,14,16,17,19] consider a simplified, two-dimensional (2D) model obtained from Eq. (2.1) via restriction of the motion to the $z = 0$ plane. The corresponding Hamiltonian is

$$H_2 = \frac{p_x^2 + p_y^2}{2} - \frac{1}{\rho} - Ff(t)\left[x\cos(\omega t + \varphi) + y\sin(\omega t + \varphi)\right], \tag{2.4}$$

with $\rho = \sqrt{x^2 + y^2}$. The 2D model is quite attractive. Consider a purely monochromatic excitation [$f(t) = 1$ for t arbitrary]. Then transformation to the frame rotating with the microwave frequency ω [29,16,17] makes the Hamiltonian time independent. The system is effectively two-dimensional (with phase space dimension $N = 4$) and the standard tools of classical dynamics (such as Poincaré surfaces of section [30]) working for $N = 4$ may be utilized. Of course, for the smooth $f(t)$ considered here, this is no longer valid.

One may remove the singularity of the Coulomb potential in (2.4) by passing to the semiparabolic coordinates, in analogy to studies of the hydrogen atom in a strong homogeneous magnetic field [28]. Define $u = \sqrt{\rho + x}$ and $v = \sqrt{\rho - x}$. Making an additional, nonlinear time transformation to the "local" time defined by $dt/d\tau = u^2 + v^2 = 2\rho$ allows us to write the Hamiltonian of the 2D model in the form

$$\mathcal{H}_2 = 2 = \frac{p_u^2}{2} + \frac{p_v^2}{2} - E(u^2 + v^2) - Ff[t(\tau)](u^2 + v^2)\left\{\frac{u^2 - v^2}{2}\cos[\omega t(\tau) + \varphi] + uv\sin[\omega t(\tau) + \varphi]\right\}, \tag{2.5}$$

where E is the energy of the system. The Hamiltonian $\mathcal{H}$ describes a system of two harmonic oscillators (with common frequency $\sqrt{-2E}$ for $E < 0$) coupled in a nonlinear way via explicitly time-dependent perturbation. As a result, the energy of the system is not conserved (after all we want to study excitation of the system), so to write the equations of motion one must pass to the extended phase space [30] creating a momentum $p_t = -E$ conjugate to t.

The presented approach, used previously also in one-dimensional studies of ionization in LPM [31], while looking a bit complicated, has two distinct advantages. First, the Coulomb singularity is removed, enabling accurate numerical integration. Second, a selection of the initial conditions corresponding to a chosen initial hydrogen state becomes very simple. The Hamiltonian of two coupled harmonic oscillators can be easily put into the form of action-angle variables and the angles may be selected uniformly and randomly to produce a statistically significant sample of initial conditions.

For a full 3D case, Eq. (2.1), the semiparabolic coordinates (defined in terms of r not ρ; see [28]), are not a good choice since the CPM problem is not axially symmetric (like the LPM ionization [7] or a static magnetic field [28]). To remove the Coulomb singularity one must exploit the full SO(4) symmetry of the hydrogen atom [32–34]. The four-dimensional coordinates may be defined as

$$\begin{aligned} s_1 &= s\cos\alpha\cos\beta, \\ s_2 &= s\cos\alpha\sin\beta, \\ s_3 &= s\sin\alpha\cos\gamma, \\ s_4 &= s\sin\alpha\sin\gamma \end{aligned} \tag{2.6}$$

and are related to standard spherical coordinates as $s = r^{1/2}$, $2\alpha = \Theta$, and $\beta + \gamma = \varphi$ (equivalently one could take the difference of β and γ [33]) via the Kustaanheimo-Stiefel (KS) transformation [35]. Thus $r = \sum_1^4 s_i^2$. The coordinates s_i (2.6) and their corresponding momenta $p_i = ds_i/dt$ obey standard Poisson bracket $\{s_i, p_j\} = \delta_{ij}$. By the nonlinear time transformation $dt/d\tau = 4r$ the Hamiltonian (2.1) may be transformed into an equivalent system of four coupled harmonic oscillators with a common frequency $2\sqrt{-2E}$:

$$\mathcal{H}_4 = 4 = \sum_{i=1}^{4}\frac{p_i^2}{2} - 4Er - 8rFf[t(\tau)]\left\{(s_1s_3 - s_2s_4)\cos[\omega t(\tau) + \varphi] + (s_2s_3 + s_1s_4)\sin[\omega t(\tau) + \varphi]\right\}, \tag{2.7}$$

where momenta (we use the same notation for brevity) are now equal to velocities with respect to a local time τ. The KS transformation to four dimensions involves an additional constant of motion in the enlarged phase space, namely,

$$\mathcal{L} = l_{12} - l_{34} = (s_1p_2 - s_2p_1) - (s_3p_4 - s_4p_3) = 0, \tag{2.8}$$

which is the difference of angular momenta of the motion projected onto (1,2) and (3,4) planes.

As far as we know, ours is the first application of the full KS transformation in the classical study of the hydrogen atom. Note also that the restricted 2D case discussed above is obtained by identifying the motion in the (1,2) plane with that in the (3,4) plane via $u = 2s_1 = 2s_3$ and $v = 2s_2 = 2s_4$ and transforming in the linear way the local time τ.

Finally, in order to follow the trajectory of electron in the CPM field, we pass, as before, to the extended phase space. The resulting dimension of the phase space is 10 (with coordinates s_i, t). The increase of the problem dimensionality is rewarded by the removal of the Coulomb singularity. The gain is both in the numerical accuracy and in the integration speed since the motion is now smooth and devoid of the strong singularities.

III. IONIZATION THRESHOLD DEPENDENCE ON FREQUENCY

In the typical numerical simulations [2] of experiments in the LPM ionization [1,9,10] a microcanonical distribu-

tion of initial conditions was assumed. This choice originated from the nature of the experiment itself, in which the principal quantum number of initial states was well defined, however, due to the mechanism of initial state preparation, a mixture of different l, m states entered the interaction region. For different reasons, such a microcanonical distribution is appropriate for classical simulation of ground-state ionization [27]; here the quantum uncertainties are relatively large.

Of course much more information on the nature of the ionization process is obtained when we have control over the initial state. We assume, therefore, an experimental situation in which initial states are preselected, i.e., have definite quantum numbers l, m. In the semiclassical limit (which should be valid for states with large quantum numbers) this leads to initial conditions chosen uniformly on an appropriate subspace of the energy shell, namely, that corresponding to the definite values of actions representing the total angular momentum and its z-axis projection [36]. Then the equations of motion resulting from the Hamiltonian Eq. (2.7) are integrated, assuming a given pulse shape and its duration. At the end of the pulse we determine final energies of electrons; the positive values correspond to the ionization. The ionization probability is then estimated as the ratio of ionized electrons to the total number of initial conditions. For situations in which the classical motion is indeed two dimensional, we use the simplified 2D Hamiltonian, (2.5) to avoid integrating the same equations twice. We have verified that appropriate trajectories obtained using (2.5) and (2.7) are the same in real space.

Let us begin with the ionization of initial circular states since this problem has been already addressed both classically [17,20] and quantum mechanically [18] in the low-frequency limit. To simulate the circular state we generate the initial conditions on the circular orbit ($l = m = 1$ at initial energy $E = -1/2$) located in the plane coinciding with the microwave polarization plane. In such a configuration we may use the restricted 2D Hamiltonian. As discussed previously [17,19] in the $|\omega| < 0.4$ regime (recall that the sign of ω determines the sign of the CPM), the definition of the ionization threshold is straightforward since for lower values of the microwave maximal amplitude F no ionization occurs, while at and above the threshold value all trajectories ionize. This is an indication of the predominantly regular motion and the ionization process resulting from the sudden breakup of a given torus (or rather the periodic orbit into which an initial circular orbit evolves) [18,20]. The situation is different at larger frequencies $|\omega| > 0.4$. Here the fraction of ionizing trajectories changes smoothly between zero and one over a significant range of the field values, resembling the behavior observed for diffusive ionization in LPM. We define, therefore, the threshold (for a given pulse shape and its duration) as the CPM amplitude F at which 10% ionization occurs.

Figure 1 presents the ionization thresholds obtained for a smooth, sine-squared pulse of duration T equal to 50 microwave periods (open symbols) and 500 microwave periods (filled symbols). At first glance the resulting curves are symmetric with respect to $\omega = 1$, which corresponds to resonance between the electron and the field (in the frame rotating with the frequency of the field the electron is at rest). The symmetry is broken by the step-like behavior around $\omega = 0$ (for a detailed discussion of this interesting behavior we refer the reader to previous works [17,20,18,19]). Similarly a sharp minimum in the ionization threshold at $\omega = -1$, corresponding to the "antirotating" situation, has no counterpart at positive frequencies.

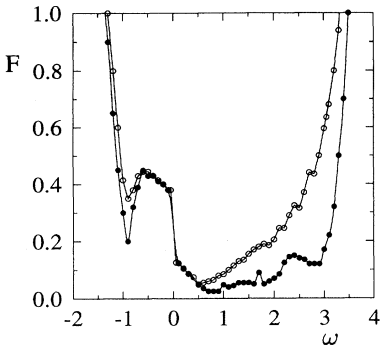

FIG. 1. Scaled 10% ionization threshold field amplitude F (scaled microwave amplitude for which 10% of the atoms ionize during the interaction time) versus scaled frequency ω of the microwave "adiabatic" pulse applied. Initial conditions are chosen on a circular orbit, coinciding with the polarization plane (the 2D Hamiltonian model is exploited here). Open dots represent data for the pulse time $T = 50$ cycles of external field and $\tau = 25$ [sine-squared pulse; see Eq. (2.2)]. Filled dots refer to $T = 500$ external field periods (the same switch on-off time τ). Lines are drawn to guide the eye. For further discussion, see the text.

It seems that the ionization process has a quite different character in various frequency regimes. In the small frequency regime $|\omega| < 0.4$, the threshold is independent of the pulse duration [19]. That confirms the interpretation of the ionization threshold as being determined by a final breakup of a regular structure embedded in the chaotic phase space (which corresponds, as we shall show below, to points originating from elliptic initial orbits). For higher frequencies the threshold field becomes dependent on pulse duration, which suggests a diffusive character of excitation, as suggested before [4,16]. For sufficiently long pulses the threshold should again be independent of the pulse duration and determined by the breakup of last invariant curves. Indeed for pulses longer than $T = 500$ cycles (not shown), the dependence on the pulse duration becomes weaker as tested for a few chosen frequency values.

The sharp increase of the threshold value for high frequencies $|\omega - 1| > 2$ is also worth noting. It occurs when the relative frequency of the field and that of the electron initial motion are greatly mismatched.

The global features of the ionization threshold frequency dependence are to some extent dependent on the orientation of the circular state with respect to the polarization plane. Suppose that the initial circular state is prepared not in the plane of light polarization, but

at some angle with respect to it. Since our coordinate frame is fixed with respect to field orientation, this will correspond to $l = 1$ and $m < 1$ values of the angular momentum and its projection onto the axis perpendicular to the polarization plane. In Fig. 2 results of the simulation obtained for $m = 1/\sqrt{2}$ (corresponding to the angle $\theta = \pi/4$ between the polarization plane and the plane defined by the circular orbit) are presented. The sharp increase of the ionization threshold for high (in absolute values) frequencies still dominates the picture, which, however, becomes more symmetric with respect to $\omega = 0$. This is easily understood, keeping in mind that no differences exist between the two types of circular polarization (i.e., the sign of ω becomes irrelevant) for the orbit perpendicular to the polarization plane ($\theta = \pi/2$). That explains also the less significant asymmetry around $\omega = 0$, as discussed in detail elsewhere [20]. Note that the antirotating resonance is still quite significant.

A. High-frequency behavior

The stabilizing effect observed for high frequencies is quite spectacular. Is it a characteristic feature of circular initial states only? Consider an elliptic initial "state" ($l = m = 0.66$) again located in the polarization plane (Fig. 3). Although the threshold still increases as a function of the field, the effect is significantly smaller and decreases with increasing state eccentricity $\epsilon = \sqrt{1 - l^2}$. Similarly, the high-threshold feature may be destroyed by considering not a slowly varying in amplitude "adiabatic" pulse but a "square" pulse as shown in the same figure. Since such a pulse is extremely nonadiabatic, during the turn on of the pulse the initial distribution of points is strongly modified. The obtained threshold behavior strongly resembles that observed for elliptic states.

The influence of the pulse shape and initial electronic state on the ionization probability is illustrated further in Fig. 4. The frequency chosen ($\omega = 2.2$) is at the border of the "high-frequency regime" and the "diffusive regime" (see below). Note big differences between different curves

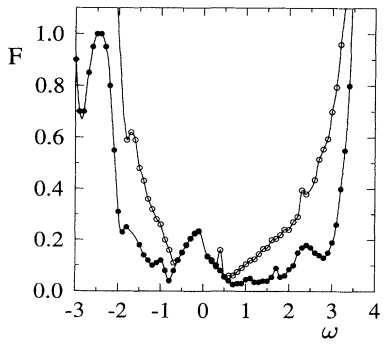

FIG. 2. Same as in Fig. 1, but initial conditions are chosen on a circular orbit positioned at angle $\Theta = \pi/4$ to the polarization plane (results of fully 3D calculations). Open dots depict data for the pulse time $T = 50$ cycles of external field and $\tau = 25$ (sine-squared pulse). Filled dots refer to $T = 500$ external field periods (the same switch on-off time τ).

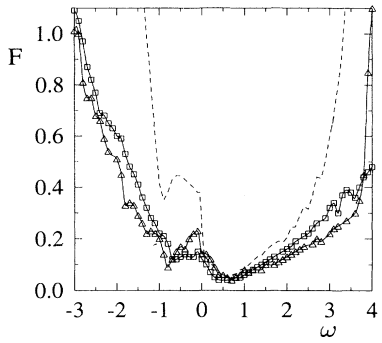

FIG. 3. Same as in Fig. 1, but different initial conditions and pulse shapes are applied. Squares refer to initial circular states ($l = 1$) in the presence of a sharply rising pulse ($\tau = 0.1$) of length $T = 50$; triangles denote a 10% threshold field for a smooth pulse ($\tau = 25$) of the same length, but initial conditions are placed on elliptical orbits ($l = 0.66$). The reference broken line stands for the case of the adiabatic (sine-squared $\tau = 25$) pulse of length $T = 50$ with circular initial states (compare Fig. 1).

for low F (i.e., close to the ionization threshold). The difference becomes less pronounced for higher fields when the ionization probability is quite large. In particular note that curves corresponding to different turn-on times τ practically coincide. This is easily understood bearing in mind that for a fixed τ, the field amplitude changes faster during the rise of the pulse for larger maximal amplitudes. Thus a "slowly rising" pulse changes into the nonadiabatic one for strong enough F.

Interestingly, notice that the ionization probability does not reach unity but rather saturates at a slightly lower, independent of the initial state and pulse shape, value. This suggests the existence of stable trapping regions for high field amplitudes and is reminiscent of the so-called "stabilization" effect [37] observed also in clas-

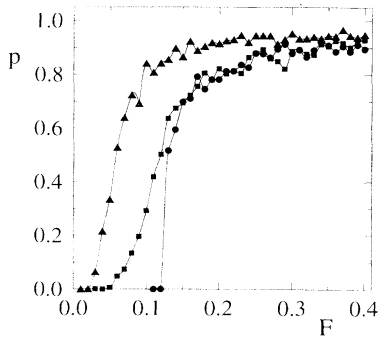

FIG. 4. The influence of the pulse shape and the initial conditions on the probability ionization p, for a fixed scaled microwave frequency $\omega = 2.2$ (the 2D Hamiltonian model is applied). In each case, the length of the pulse of the maximal scaled amplitude F is $T = 500$; dots represent data for circular initial states and adiabatic pulse ($\tau = 25$), triangles the same pulse and elliptical ($l = 0.66$) initial conditions, and squares the sharply rising ($\tau = 1$) pulse and circular initial states. For further description, see the text.

sical simulations of ionization in linearly polarized radiation [27].

The increase of the ionization threshold with frequency for sufficiently large $|\omega|$ values is quite understandable if we consider the system as a set of two coupled oscillators, the nonlinear oscillator (the atom) and the electromagnetic field mode. The huge frequency difference allows then for the adiabatic averaging over the "fast motion," which leads to an effective atomic potential for the "slow motion." The averaging procedure is best carried out in the Kramers-Henneberger frame [38,37] in which the nucleus oscillates with the field frequency. Under the condition $\alpha = F/\omega^2 < 1$ one can expand the potential in the power series and average over the fast motion using the Kapitza method [39]. A similar approach has been used for linearly polarized microwave excitation of high angular momentum states [41]. The resulting effective potential is radially symmetric

$$V_{\text{eff}} = -\frac{1}{r} - \frac{\alpha^2}{r^3} + \frac{5\alpha^2}{2\omega^2}\frac{1}{r^6} - \frac{7\alpha^2}{4\omega^4}\frac{1}{r^9} + O(\alpha^4). \quad (3.1)$$

Thus the motion in the effective potential is strictly integrable (angular momentum is conserved). As long as the coupling with fast variables is weak, no excitation occurs. Figure 5 illustrates the fate of different trajectories in rather strong fields, but for a relatively small α. Excitation, or possible ionization as in Fig. 5(c), occurs when the coupling between slow oscillations (Kepler-like motion) and fast motion (epicycles) occurs, i.e., when small loops degenerate into cuspid curves. Note that the excitation process may take place far from the nucleus, contrary to some predictions [16]. This behavior is the opposite of the one observed for low angular momentum states in classical LPM ionization (the so-called chaos border [4]). In the latter case the collisions with the nucleus lead to an efficient excitation mechanism of diffusive character.

By the same mechanism classical calculations of ionization for purely Coulombic systems may overestimate the ionization probability and lead to an underestimation of stabilization for linearly polarized excitation [27]. On the contrary, for CPM, the threshold amplitude values obtained in classical calculations for large $|\omega|$ should significantly overestimate the quantum predictions in the case of circular states except, maybe, for very large principal quantum numbers n. The semiclassical wave function corresponding to a circular state is localized in the vicinity of the circular orbit in the "toruslike" form of finite thickness. As a result, the semiclassical simulation of the ionization process [36] should include, in principle, the average over orbits with different eccentricities (confined to the interval dependent on n) and over initial orbit orientations with respect to the polarization plane [according to the distribution related to the corresponding harmonic $P_l^n(\cos\theta)$]. Such an average would (as follows from results shown in Figs. 2 and 3) lower the threshold value for circular states. On the basis of classical simulations we may expect also a significant dependence of the threshold on the shape of the microwave pulse (and in particular its rise time) in quantum studies.

B. Diffusive ionization regime

As mentioned above the dependence of the ionization threshold on the pulse duration for $\omega > 0.4$ suggests that the ionization takes place in the diffusive manner in this regime. One expects, therefore, that below a cer-

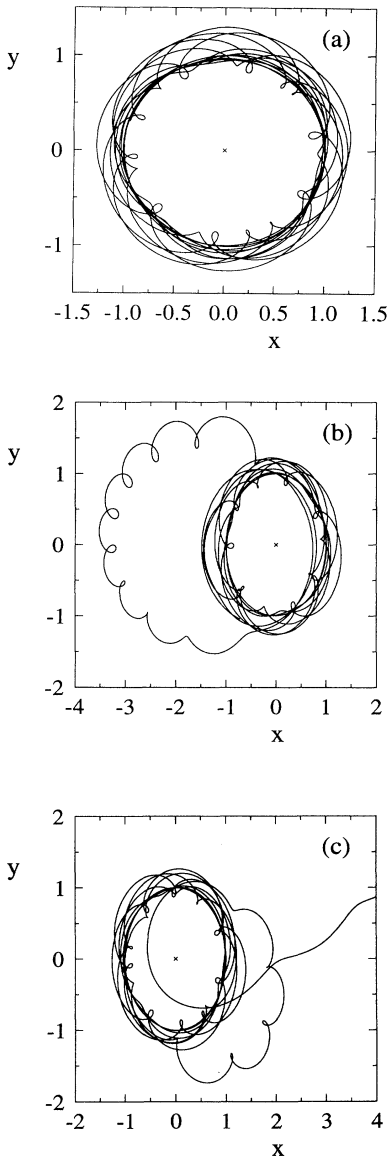

FIG. 5. Classical orbit of the electron in the (x, y) plane (2D simulations) for high field frequency $\omega = 4$ and strong short sine-squared pulse ($T = 50$, $\tau = 25$) of the maximal amplitude $F = 4.5$ ($\alpha = 0.28125$). Each panel presents the electron trajectory during the pulse time for one initial condition chosen on a circular orbit. (a) and (b) present examples of nonionizing orbits and (c) shows the ionization process at the end of the pulse, i.e., when the field amplitude is much smaller than the maximal amplitude. The cross depicts the position of the nucleus. Note that in each case, even when ionization occurs, the trajectory passes far away from the nucleus.

tain frequency- *and* initial-state-dependent threshold the motion in the phase space is regular. Above the threshold, when the maximal microwave field amplitude exceeds a certain value, a diffusive gain of electron energy (or rather the corresponding action; see below and [4]) occurs. The amount of energy gained for a single electron should be strongly dependent on the initial conditions. To characterize the resulting distribution, we define, in the obvious analogy to quantum mechanics, the "quantum number" n (which is also one of the classical actions [4]) via $E = -1/2n^2$ for a given energy E. Recall that initially we take $E = -1/2$ corresponding to $n = 1$; thus the initial n distribution is δ peaked at $n = n_0 = 1$. The atom is then excited by a smooth sine-squared pulse of duration $T = 500$ cycles. We monitor the energy (and n values) of electrons during the pulse excitation. Actually, to store less data, only first and second moments of the resulting distribution are collected. The moments are defined in an obvious way:

$$m_1(t) = \langle n(t) - n_0 \rangle,$$
$$m_2(t) = \langle (n(t) - \langle n(t) \rangle)^2 \rangle / n_0^2 \,. \tag{3.2}$$

Above the threshold, a finite fraction of electrons gets ionized and the corresponding n values are not defined. Such events are excluded from the calculation of moments. To avoid large local fluctuations (when an electron passes through very large n values before leaving the atom) we include on the average only trajectories with $n(t) < 10$.

Let us begin our discussion with initial circular states. A typical "below threshold" behavior is depicted in Fig. 6. Figures 6(a) and 6(b) represent the first and the second moment, respectively. Note that although the electron gains some energy in the microwave field (the ponderomotive contribution is eliminated), it gives back the energy to the field and returns to the *same* initial orbit. Note how nicely the dispersion (second moment) comes back to zero after the pulse has passed. Let us stress that such a behavior is typical for smooth pulses only, when the atom can adapt to changes of the microwave field amplitude (see also below).

A typical "diffusive excitation" example is presented in Fig. 7 for the same maximal field amplitude but a slightly smaller frequency. Note that in this case, electrons on average gain some energy after the pulse has passed [first moment in Fig. 7(a)], but the resulting distribution is not concentrated at some n value [compare the second moment in Fig. 7(b)].

The diffusion process is strongly frequency dependent, as exemplified in Fig. 8 for longer pulses. To facilitate the comparison we adjusted the maximal field amplitudes to have similar ionization probabilities (to partially eliminate the influence of the frequency-dependent threshold). The figure shows a quite typical behavior for $\omega > 1$, namely, the slowing down of the diffusion with increasing frequency. The estimates of the diffusion coefficient dependence on the frequency and field amplitude have been obtained for monochromatic fields only [4]. We do not attempt to determine the "effective" coefficients for smooth pulses since this would require much more extensive numerical studies.

In fact, the excitation process is strongly dependent on the pulse shape. Assume a rectangular pulse shape, for which we choose the unrealistic switch on-off time $\tau = 0.1$, keeping other parameter values the same as for the below threshold behavior presented in Fig. 6. The results (Fig. 9) show a strong diffusive excitation. The huge difference between Figs. 6 and 9 (in both cases electrons were initially localized on a circular orbit) can be explained only by the fact that for a sharply rising pulse, electron motion becomes strongly distorted and loses its memory about the initial orbit (the electron is "kicked" into a different phase-space region). This idea can be verified by analyzing the excitation process of initially elliptic states (Fig. 10). The results indicate that indeed such states (orbits) become significantly excited in the diffusive manner for the same frequency, but for a smaller value of the maximal field amplitude to compensate for the faster excitation process. Thus the circular

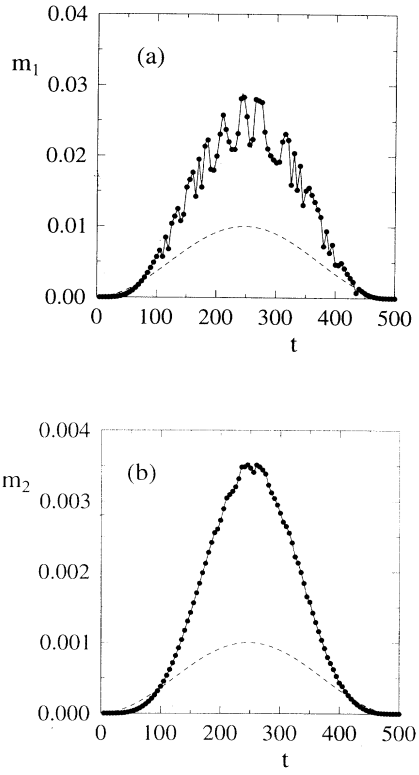

FIG. 6. Statistical moments (a) m_1 and (b) m_2 [see Eq. (3.2)] of the ensemble of initial circular state conditions as a function of the interaction time t (the 2D model is assumed). The broken line shows the shape of the (sine-squared) pulse of maximal amplitude $F = 0.1$ and duration $T = 500$ external field cycles ($\tau = 250$). This is "below threshold" behavior. A field frequency $\omega = 2.2$ and 1000 initial conditions were taken. The energy of the electron (pondermotive energy is excluded) is transformed into an equivalent principal quantum number $n(t)$. Each orbit during the interaction time fulfills the condition $n(t) < 10$. For a more detailed description, see the text.

and low eccentricity states are more resistant to excitation than the elliptic states. Here our numerical study confirms the predictions obtained on the basis of the resonance overlap criterion by Howard [16]. Note, however, that elongated, high eccentricity states ($l = m = 0.01$) are less excited than typical elliptic states ($l = m = 0.5$); thus the excitation mechanism cannot be unambiguously linked solely to collisions with the nucleus (as often suggested in the literature).

Finally, Fig. 11 presents typical results obtained in the fully three dimensional model in the diffusive regime. As intuitively expected, the diffusion is slower with an increasing angle between the orbit and the polarization plane. This supports the claim [16] that ionization thresholds for arbitrary states may be well approximated in a 2D model. The effect of the external field is strongest if the initial orbit coincides with the polarization plane.

C. "Negative" frequencies regime

Recall that, in our notation, "negative" frequencies correspond to the case of negative m values when the electron rotates in the opposite direction to the CPM field. For small ω the motion is mainly regular and the ionization threshold is independent of the pulse duration [17]. For larger (in the absolute sense) frequencies, first the region dominated by the pronounced antirotating resonance at $\omega = -1$ is reached and then the threshold field values increase sharply (compare Fig. 1). The latter effect appears since the relative frequency between the field and the electron motion becomes large. Thus the region of typical diffusive excitation, with a slow dependence of the ionization probability on the maximal field amplitude, practically disappears, at least for circular states lying in the CPM polarization plane. Instead one observes a quite sharp threshold behavior of the ionization probability (see Fig. 12) similar to that observed for high positive frequencies (compare Fig. 4).

The appearance of a strong resonance at $\omega = -1$ (or rather a field shifted value of $\omega \approx -0.9$) in the form of a deep dip in the threshold frequency behavior is due to a 1:1 resonance between the electron and the field which

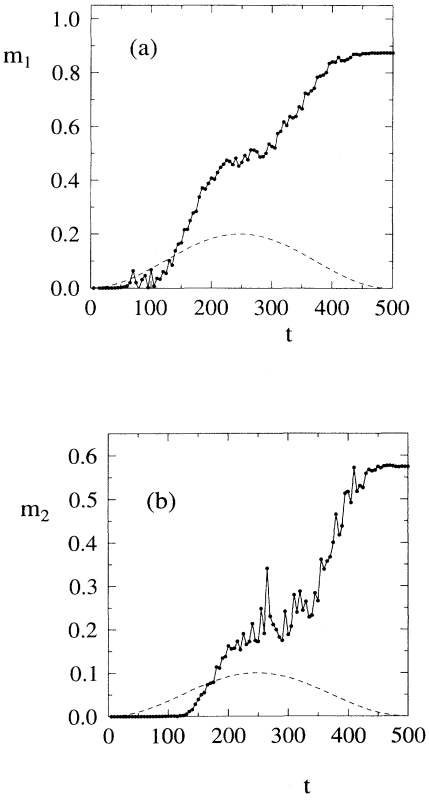

FIG. 7. Same as in Fig. 6, but for a slightly smaller field frequency ($\omega = 1.9$); the maximal field amplitude is the same. Note that (a) after the pulse has passed, electrons on average gain some energy; the distribution is smear out over a vast region of n values [(b) note the considerable final second moment]. In this case 696 initial conditions out of 1000 lead to excitation $n(t) > 10$.

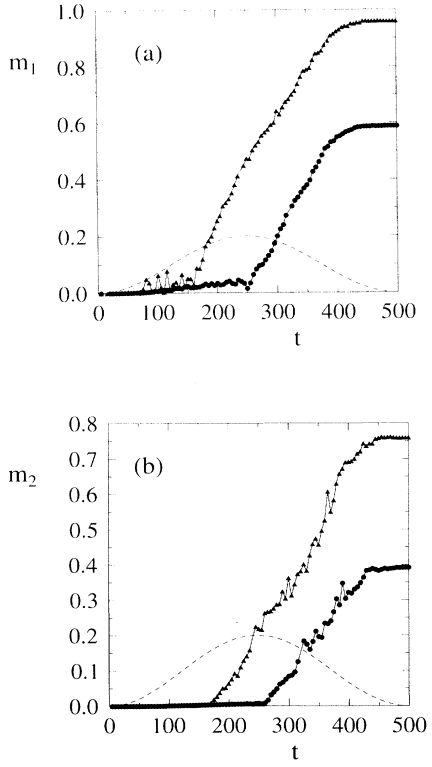

FIG. 8. (a) First and (b) second statistical moments for the field frequency $\omega = 1.9$ and the maximal field amplitude $F = 0.07$ (triangles) and $\omega = 2.2$ and $F = 0.13$ (dots). There is an assumed sine-squared pulse (the broken line shows its shape in time) and circular initial conditions (the 2D model is used). The field amplitudes have been taken to achieve approximately the same ionization probability during the interaction with the pulse ($p \approx 0.04$). For $\omega = 1.9$, 220 out of 1000 initial conditions were recorded, leading to the excitation $n(t) > 10$; for $\omega = 2.2$ there were only 159 such initial conditions. For further discussion, see the text.

facilitates excitation. The resonant behavior is amplified since it is surrounded by two relatively stable regions of small absolute frequencies and a large ω shoulder. A comparison of Figs. 2 and 3 shows that this feature is quite insensitive to perturbations and therefore should be possible to observe experimentally under the condition of selective initial-state preparation (which is not an easy task).

The comparison between Figs. 1 and 2 reveals another interesting feature of the negative frequency regime. For an angle $\Theta = \pi/4$ between the plane of a circular initial orbit and a polarization plane (Fig. 2) one can observe well pronounced resonance for $\omega \approx -2.9$ (this corresponds to $m = -1/\sqrt{2}$ and field frequency $\omega \approx 2.9$). This deep resonance, which may be attributed to a 3:1 resonance between the field frequency and the electron, is absent for the case when the orbit plane coincides with the polarization plane (compare Fig. 1).

D. "Stabilization windows"

There has been much discussion recently about possible mechanisms of "stabilization," i.e., a decrease of the ionization probability with the increasing field amplitude. One of the mechanisms, commonly called the adiabatic stabilization [37], is characterized by a stable decrease of the ionization rate with the field amplitude (for sufficiently large frequencies) after a state-dependent threshold field value has been reached. The effect is quite pronounced when studied in the field-dressed (Floquet) basis as a property of a single state uniquely (adiabatically) evolving from the field-free atomic state. It remains an open question to what extent the realistic pulse excitation will allow for a sufficient population of a single Floquet state to observe the effect and whether the atom will not ionize earlier during the pulse rise [40].

The second mechanism, called the dynamic stabilization, may occur for short laser pulses. If during the pulse rise the atom is excited to a high-lying state, the electronic wave packet may leave the vicinity of the nucleus (where further energy absorption is possible) and return only after the pulse had died away [45,46]. Such a behavior is typically characterized in the ionization dependence on the pulse amplitude by stabilization windows [finite intervals of negative $dp(F)/dF$], i.e., dips causing a nonmonotonic increase of $p(F)$. Similar behavior may

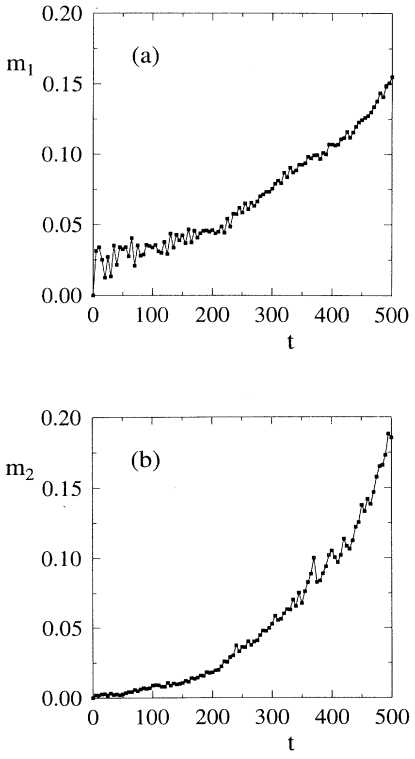

FIG. 9. Same as in Fig. 6 (again $\omega = 2.2$), but for a sharply rising pulse ($\tau = 0.1$) of maximal amplitude $F = 0.05$; the initial conditions are located on the circular orbit. Only 19 out of 1000 initial orbits have been rejected in the statistical moments' evaluation.

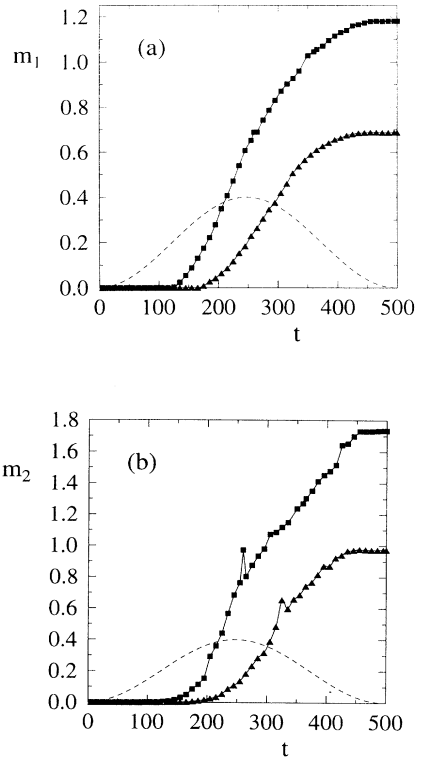

FIG. 10. Time evolution of the statistical moments for elliptic initial states located in the polarization plane: $l = 0.01$, triangles; $l = 0.5$, squares. The broken curve depicts the shape of the sine-squared pulse of maximal amplitude $F = 0.05$ and frequency $\omega = 2.2$. A smaller value of F (compare Figs. 6 and 9) was taken to compensate for the more efficient excitation in the case of elliptic initial conditions . In the simulations for each value of l, 2000 initial values have been taken. For $l = m = 0.5$, 538 trajectories ended up above $n = 10$, whereas for a much smaller value $l = m = 0.01$, there were only 114 such cases. For further discussion, see the text.

occur classically [27].

The latter mechanism is quite frequent in our classical simulations of circularly polarized excitation. The typical classical trajectory exemplifying this case has been shown in Fig. 5. While the data have been obtained for a longer pulse and the electron managed to return sufficiently close to the nucleus to undergo deexcitation [Fig. 5(b)] or subsequent ionization [Fig. 5(c)], for a sufficiently short pulse it would have remained in the bound excited state in both cases.

It is worth stressing that a quite similar behavior, i.e., nonmonotonic behavior of the ionization probability as a function of the pulse amplitude, may be observed in a completely different frequency and intensity regime—for microwave ionization in both linearly and circularly polarized radiation. In LPM this behavior, sometimes referred to as "subthreshold" peaks, has been noted both for $\omega < 1$ [42] and for $\omega > 1$ [43] and discussed in detail [7]. It may be correlated with the sensitive dependence

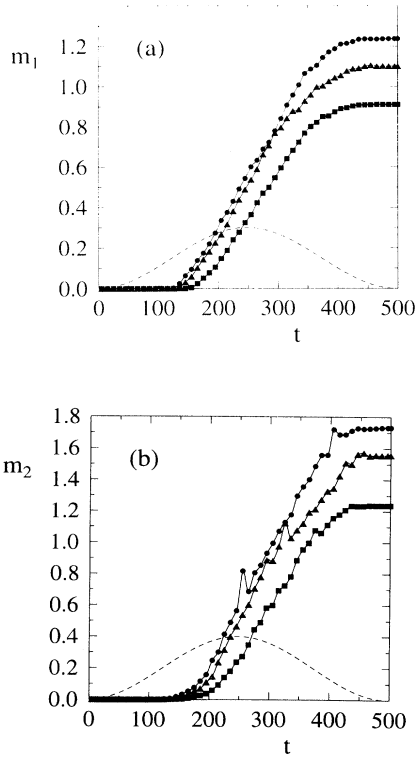

FIG. 11. Statistical moments for the 3D model. A sine-squared pulse of maximal amplitude $F = 0.05$ was assumed. Initial conditions lie on an elliptic orbit $l = 0.5$. Dots represent data for the case when an initial orbit lies in the polarization plane ($m = l = 0.5$) and triangles and squares refer to data obtained for initial orbits at angle with the polarization plane such that the projection of angular momentum m is equal, respectively, to 0.4 and 0.2. The numbers of rejected orbits during the simulations are 288, 176, and 80 for m=0.5, 0.4, and 0.2, respectively. There were 1000 initial conditions in each case. The broken line represents the pulse shape in time. (a) shows the first moment and (b) the second one during the interaction time.

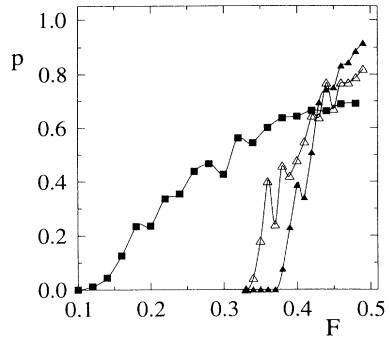

FIG. 12. Ionization probability p versus maximal field amplitude F of the sine-squared pulse ($\tau = T/2$) for $T = 50$ external field cycles (short pulses). Triangles show the dependence for negative frequencies, filled triangles are for $\omega = -0.8$, and open symbols for $\omega = -0.9$. Filled squares denote data for $\omega = 1.5$. Here 500 circular initial conditions have been taken for each case.

of Floquet state widths on field amplitude due to abundant avoided crossings in the partially chaotic regime or classically to the presence of field-dependent resonances and other quasiregular structures in the phase space.

A typical situation is presented in Fig. 13. Note a strongly nonmonotonic behavior of the ionization probability for $\omega = 1.2$, strongly dependent on the pulse duration. This suggests that the structures responsible for such a behavior are not a stable islands (in which case one would rather expect a trapping of a certain portion of initial conditions inside such a structure independently of the pulse duration) but rather quasiregular bottlenecks for transport preventing the excitation (and ionization). A different situation occurs for $\omega = 1$, where presumably a stable secondary resonance island existing for the $F \in [0.04, 0.06]$ interval is responsible for a pronounced plateau, which is quite insensitive to the pulse duration.

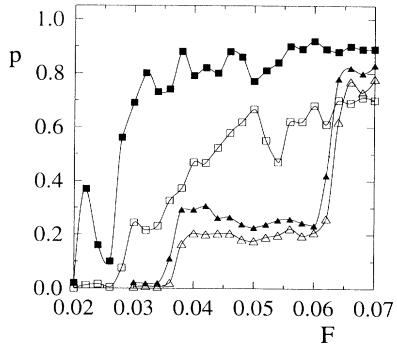

FIG. 13. Ionization probability p dependence on maximal field amplitude F. Here "flat-top" long pulses are applied (open symbols, T=500 in Kepler units; filled symbols, $T = 1500$ in Kepler units). In each case, the turn on-off time $\tau = 50$ in Kepler units. Triangles represent data for $\omega = 1.0$ and squares show data for a slightly greater frequency, namely, $\omega = 1.2$. Note that for $\omega = 1.0$ there are no significant differences between results for pulses of different lengths. For further discussion, see the text.

Let us note here that such an atypical $p(F)$ behavior suggests strongly nonexponential decay. In fact, one may observe in such a case an algebraic decay curve by looking at the dependence of the ionization probability [or rather the survival probability $s(T) = 1 - p(T)$] on pulse duration T as discussed for a simplified linear polarization case [44] and also for CPM [47].

It should be stressed that the mechanism leading to stabilization windows for relatively weak (just above the threshold value) field amplitudes and practically arbitrary frequency (except for the low-frequency "regular" regime) is distinctly different from the typical short and strong pulse stabilization window. In the chaotic ionization, the effect appears for sufficiently long interaction times such that the presence of quasiregular structures in field distorted phase space may determine the electrons' fate. For short strong pulses such a picture loses its meaning as the field amplitude changes too fast in time.

IV. CONCLUSION

The aim of this, primarily numerical, study has been to study in detail the classical features of ionization of atoms by circularly polarized radiation. In this sense this work both extends the previous classical investigations [13,14,16,17,19] into different frequency regimes and supplements mostly analytical studies [13,14,16,19].

Our simulations indicate that there are practically three frequency regimes: a low-frequency regime with predominantly regular behavior [17–19], a diffusive chaotic regime of intermediate frequencies, and a high-frequency regime where the atoms are more resistant to ionization and where a regular motion also persists for fields below the ionization threshold. In agreement with resonance overlap based predictions [16] we have found that circular states are most resistant to CPM perturbation. Typically the states most vulnerable to ionization are the states of intermediate quantum numbers oriented mostly in the polarization plane. The threshold behavior of such states should thus determine the threshold for ionization in experiments in which no initial-state selection will be attempted.

This conclusion is in some contradiction to claims that, at least for sufficiently high frequencies, the ionization takes place as a result of hard collisions with the nucleus. In fact, at least for most of the low eccentricity states intensively studied by us, although some ionization occurs in this fashion, collisions with the nucleus are not a primary mechanism of ionization. That makes a Kepler map approach [4,14] for such states quite questionable. In particular note that in marked difference with the linear polarization case [4], the ionization thresholds for all the typical situations studied here *increase* with increasing ω instead of decreasing as in a simple one-dimensional H atom classical model. On the other hand, low eccentricity states in LPM classical simulations [48] behave in a way similar to the CPM case discussed here.

The increase of the ionization threshold with frequency is particularly spectacular classically for circular states lying in the light polarization plane. As discussed above, we expect that the effect will be seriously diminished in quantum world, but nevertheless it could be quite pronounced. Its experimental verification requires, however, a state-selective initial preparation of atoms before their interaction with the microwaves. That may be quite difficult experimentally. We think, however, that both the interesting low-frequency effects [17,18] as well as the phenomena shown here (the antirotating resonance and the symmetry of high-frequency behavior with respect to $\omega - 1$) deserve to be experimentally verified, especially since measurements of the microwave ionization of atoms prepared in a well defined preselected state would deepen significantly our understanding of the chaotic ionization process also in the LPM case and would provide a new challenge for the theory.

ACKNOWLEDGMENTS

We are grateful to Dominique Delande for discussions and for permission to use computers of his group at Laboratoire Kastler-Brossel for numerical simulations. Some part of the simulations has been performed on the i860 card donated by the Alexander von Humboldt Foundation. This work was supported by the Polish Committee of Scientific Research under Grants No. 2P302 035 05 (R.G.) and No. 2P302 102 06 (J.Z.).

[1] J. E. Bayfield and P. M. Koch, Phys. Rev. Lett. **33**, 258 (1974).
[2] J. G. Leopold and I. C. Percival, J. Phys. B **12**, 709 (1979).
[3] G. Casati, B. V. Chirikov, D. L. Shepelyansky, and I. Guarneri, Phys. Rep. **154**, 77 (1987).
[4] G. Casati, I. Guarneri, and D. L. Shepelyansky, IEEE J. Quantum Electron. **24**, 1420 (1988).
[5] B. V. Chirikov, in *Chaos and Quantum Physics*, Les Houches Lectures Session LII, 1989, edited by M.-J. Giannoni, A. Voros, and J. Zinn-Justin (North-Holland, Amsterdam, 1991), p. 443.
[6] R. V. Jensen, S. M. Susskind, and M. M. Sanders, Phys. Rep. **201**, 1 (1991).
[7] A. Buchleitner, thèse de doctorat, Université Pierre et Marie Curie, 1993.
[8] M. V. Berry and K. E. Mount, Rep. Prog. Phys. **35**, 315 (1972).
[9] P. M. Koch, in *Chaos and Quantum Chaos*, Proceedings of the Eighth South African Summer School in Theoretical Physics, 1992, Blydepoort, Republic of South Africa, edited by W. D. Heiss (Springer-Verlag, Berlin, 1993).
[10] J. E. Bayfield and D. W. Sokol, in *Physics of Atoms and Molecules: Atomic Spectra and Collisions in External Fields*, edited by K.T. Taylor, M. H. Nayfeh, and C. W. Clark (Plenum, New York, 1988).

[11] J. Mostowski and J. J. Sanchez-Mondragon, Opt. Commun. **29**, 293 (1979).
[12] B. I. Meerson, E. A. Oks, and P. V. Sasorov, J. Phys. B **15**, 3599 (1982).
[13] M. Nauenberg, Phys. Rev. Lett. **64**, 2731 (1990).
[14] M. Nauenberg, Europhys. Lett. **13**, 611 (1990).
[15] J. A. Griffiths and D. Farrelly, Phys. Rev. A **45**, R2678 (1992).
[16] J. E. Howard, Phys. Rev. A **46**, 364 (1992).
[17] K. Rzążewski and B. Piraux, Phys. Rev. A **47**, R1612 (1993).
[18] J. Zakrzewski, D. Delande, J. C. Gay, and K. Rzążewski, Phys. Rev. A **47**, R2468 (1993).
[19] P. Kappertz and M. Nauenberg, Phys. Rev. A **47**, 4749 (1993).
[20] D. Delande, R. Gębarowski, M. Kuklińska, B. Piraux, K. Rzążewski, and J. Zakrzewski, in *Super-Intense Laser-Atom Physics*, Vol. 316 of *NATO Advanced Study Institute, Series B: Physics,* edited by B. Piraux, A. L'Huillier, and K. Rzążewski (Plenum, New York, 1993), p. 317.
[21] P. Fu, T. J. Scholz, J. M. Hettema, and T. F. Gallagher, Phys. Rev. Lett. **64**, 511 (1990).
[22] T. F. Gallagher, Mod. Phys. Lett. B **5**, 259 (1991).
[23] P. M. Koch (private communication).
[24] D. Wintgen, Z. Phys. D **18**, 125 (1991).
[25] D. Delande and J. C. Gay, Europhys. Lett. **5**, 303 (1988).
[26] J. C. Day, T. Ehrenreich, S. B. Hansen, E. Horsdal-Pedersen, K. S. Mogensen, and K. Taulbjerg, Phys. Rev. Lett. **72**, 1612 (1994).
[27] M. Gajda, J. Grochmalicki, M. Lewenstein, and K. Rzążewski, Phys. Rev. A **46**, 1638 (1992).
[28] See, e.g., D. Delande, in *Chaos and Quantum Physics* (Ref. [5]), p. 665.
[29] F. V. Bunkin and A. Prokhorov, Zh. Eksp. Teor. Fiz. **46**, 1090 (1964) [Sov. Phys. JETP **19**, 739 (1964)].
[30] A. J. Lichtenberg and M. A. Liberman, *Regular and Stochastic Motion* (Springer-Verlag, New York, 1983).
[31] J. G. Leopold and D. Richards, J. Phys. B **18**, 3369 (1985).
[32] A. O. Barut, C. K. E. Schneider, and R. Wilson, J. Math. Phys. **20**, 2244 (1979).
[33] A. C. Chen, Phys. Rev. A **22**, 333 (1980); **23**, 1655 (1981).
[34] D. Delande, thèse de doctorat d'etat, Université de Paris, 1988.
[35] P. Kustaanheimo and E. Stiefel, J. Reine Angew. Math. **218**, 204 (1965).
[36] Additionally, one could average the obtained results over the distribution (e.g., Gaussian) of initial actions to simulate quantum uncertainties. Such an approach obviously violates scaling properties and is not attempted here.
[37] M. Gavrila and J. Z. Kamiński, Phys. Rev. Lett. **52**, 613 (1984); R. J. Vos and M. Gavrila, *ibid.* **68**, 170 (1992).
[38] H. A. Kramers, *Collected Scientific Papers* (North-Holland, Amsterdam, 1956), p. 262; W. C. Henneberger, Phys. Rev. Lett. **21**, 838 (1968).
[39] L. D. Landau and E. M. Lifshitz, *Mechanics* (Addison-Wesley, Reading, MA, 1960).
[40] P. Lambropoulos, Phys. Rev. Lett. **55**, 2141 (1985).
[41] F. Benvenuto, G. Casati, and D. L. Shepelyansky, Phys. Rev. A **45**, R7670 (1992); **47**, R786 (1993).
[42] R. Blümel and U. Smilansky, Z. Phys. D **6**, 83 (1987).
[43] H. P. Breuer, K. Dietz, and M. Holthaus, Z. Phys. D **18**, 239 (1991).
[44] Y.-C. Lai, C. Grebogi, R. Blümel, and M. Ding, Phys. Rev. A **45**, 8284 (1992).
[45] K. Kulander, K. J. Schafer, and J. L. Krause, Phys. Rev. Lett. **66**, 2601 (1991).
[46] K. Burnett, P. L. Knight, B. R. Piraux, and V. C. Reed, Phys. Rev. Lett. **66**, 301 (1991); V. C. Reed, P. L. Knight, and K. Burnett, *ibid.* **67**, 1415 (1991).
[47] R. Gębarowski and J. Zakrzewski, Phys. Rev. A **50**, 4408 (1994).
[48] Especially when the states are localized in the plane perpendicular to the polarization axis, as will be shown by us elsewhere.